Theory of Dzyaloshinski-Moriya antiferromagnetism in distorted CuO_2 and NiO_2 planes

Wataru Koshibae, Yukinori Ohta, and Sadamichi Maekawa
Department of Applied Physics, Nagoya University, Nagoya 464-01, Japan
(Received 22 February 1994)

Moriya's perturbation theory is applied to the distorted NiO_2 and CuO_2 planes, and the effective spin Hamiltonians are derived. Spin-wave theory is explored for the Hamiltonians, and the spin-wave excitations are studied for nickelates and cuprates with low-temperature orthorhombic and low-temperature tetragonal (LTT) structures. It is shown that in the cuprates the origin of the anisotropy responsible for the spin-wave gaps is different for in-plane and out-of-plane modes: i.e., anisotropic superexchange for the in-plane mode, and anisotropic direct exchange for the out-of-plane mode. This difference explains the observed structural dependence of the spin-wave gaps in $La_{1.65}Nd_{0.35}CuO_4$. In nickelates, the single-ion anisotropy is solely responsible for the spin-wave gaps, which are observed in La_2NiO_4. We discuss the mechanism of the weak ferromagnetism; in the nickelates the Dzyaloshinski-Moriya (DM) interaction causes the weak ferromagnetism in the LTT phase where an appropriate spin configuration is prepared by the single-ion anisotropy. In the cuprates, where the single-ion anisotropy for preparing the spin configuration is absent, the DM and pseudodipolar interactions themselves determine the spin configuration: the weak ferromagnetism originates only from the competition between these two interactions. It is proposed that a multiorbital effect is essential to explain the observed weak ferromagnetism in the LTT phase of $La_{1.65}Nd_{0.35}CuO_4$.

I. INTRODUCTION

The layered perovskite compounds, La_2CuO_4, $La_{2-x-y}Nd_ySr_xCuO_4$, and La_2NiO_4, exhibit a number of crystal structures including high-temperature tetragonal phase, low-temperature orthorhombic (LTO) phase, and low-temperature tetragonal (LTT) phase,[1-5] and associated with these structures a number of intriguing magnetic behaviors have been observed.[6-10] La_2CuO_4 shows weak ferromagnetism in the LTO phase.[6] $La_{1.65}Nd_{0.35}CuO_4$ shows weak ferromagnetism in both LTO and LTT phases.[7-9] La_2NiO_4 shows weak ferromagnetism only in the LTT phase.[10] The magnetic anisotropy is observed as the spin-wave gaps at the center of the two-dimensional Brillouin zone.[8,10,11] The spin-wave gaps with in-plane and out-of-plane modes have been reported to be 2.3 and 5 meV, respectively, for La_2CuO_4.[8] Structural dependence of the spin-wave gaps has been observed in $La_{1.65}Nd_{0.35}CuO_4$ (Ref. 8) and La_2NiO_4:[10] in both compounds the in-plane spin-wave gap depends sensitively on the structural phase transition, but the out-of-plane spin-wave gap does not. In $La_{1.65}Nd_{0.35}CuO_4$, the in-plane spin-wave gap of the LTT phase is about two times larger than that of the LTO phase.[8] In La_2NiO_4, the in-plane spin-wave gap of the LTT phase is about one half of that of the LTO phase.[10]

Several groups have recently studied the Dzyaloshinski-Moriya (DM) interaction[12,13] in the distorted CuO_2 plane.[14-18] Coffey, Bedell, and Trugman[14] have pointed out that the spatial pattern of the DM interaction must reflect the crystal symmetry correctly; an effective spin Hamiltonian has been suggested and the spin-wave dispersion has been calculated. The first attempt of microscopic derivation of the DM interaction has been made by Coffey, Rice, and Zhang;[15] they have applied Moriya's perturbation theory[13] to the cuprates. Shekhtman, Entin-Wohlman, and Aharony[16] have reexamined the Moriya's perturbation theory and have proposed that the frustration due to bond dependence of the anisotropies is the origin of the weak ferromagnetism in the LTO phase of La_2CuO_4. Bonesteel[17] has discussed the magnetism of $YBa_2Cu_3O_6$ as well. In our previous paper,[18] we have claimed that the contributions from multiorbitals of the ligand ions are essential for the emergence of weak ferromagnetism in the distorted CuO_2 plane. Shekhtman, Aharony, and Entin-Wohlman have pointed out the importance of the pseudodipolar interaction of direct-exchange mechanism in describing magnetic behaviors of cuprates.[16,19]

In this paper, we will offer a general understanding of the Dzyaloshinski-Moriya antiferromagnets by making a comparison of magnetic behaviors between cuprates, La_2CuO_4 and $La_{1.65}Nd_{0.35}CuO_4$, and nickelates La_2NiO_4. The cuprates and the nickelates differ only in their spins on the magnetic ions. Understanding of magnetic behaviors of these systems provides a good opportunity for clarifying the physics of weak ferromagnetism. We will show the following. (i) In $La_{1.65}Nd_{0.35}CuO_4$, the different structural dependence between the in-plane and out-of-plane spin-wave gaps is due to the difference in their origin: the in-plane spin-wave gap is provided by the anisotropic exchange interactions of superexchange mechanism whereas the out-of-plane spin-wave gap is provided by the anisotropic exchange interactions of direct-exchange mechanism. (ii) In La_2NiO_4 the single-ion anisotropy controls the spin arrangement: the weak ferromagnetism appears only if the spin arrangement is such that the DM interaction can provide the energy gain. (iii) The spin-wave gaps are provided solely by the

0163-1829/94/50(6)/3767(12)/$06.00

single-ion anisotropy in La_2NiO_4: this explains the different structural dependence of the in-plane spin-wave gap between nickelates and cuprates.

The essence of the Dzyaloshinski-Moriya antiferromagnetism manifests itself in the comparative discussion on the magnetism of cuprates and nickelates. The spatial pattern of the DM interaction is determined by the crystal structure. The spin arrangement is fixed by the single-ion anisotropy because the strength of the single-ion anisotropy overwhelms the strength of the anisotropic exchange interactions of both superexchange and direct-exchange mechanisms. The weak ferromagnetism is realized when the spin system can obtain the energy gain by laying the fixed spin arrangement in accord with the determined spatial pattern of the DM interaction. The weak ferromagnetism in ordinary Dzyaloshinski-Moriya antiferromagnets, e.g., α-Fe_2O_3, $MnCO_3$, $CoCO_3$, CrF_3, etc., emerges in spin systems which involve single-ion anisotropy. In the ordinary Dzyaloshinski-Moriya antiferromagnets, the DM interaction cannot be detected in the magnetic properties such as weak ferromagnetism and spin-wave gaps if there is no cooperation of the single-ion anisotropy.

The weak ferromagnetism of cuprates is quite peculiar because the single-ion anisotropy does not exist in this system. In this sense cuprate is not one of the ordinary Dzyaloshinski-Moriya antiferromagnets; its weak ferromagnetism requires explanation from a different mechanism. The problem is to provide a mechanism of constructing the spin arrangement in which the DM interaction can contribute to the gain in energy of the spin system. We propose that the multiorbital effect is essential for the emergence of the weak ferromagnetism in the LTT phase of $La_{1.65}Nd_{0.35}CuO_4$.

In Sec. II, we explore Moriya's perturbation theory in the NiO_2 and CuO_2 planes of the LTO and LTT phases, and we derive the anisotropic exchange interactions of superexchange mechanism. The anisotropic exchange interactions of direct-exchange mechanism is derived for the NiO_2 and CuO_2 planes in Sec. III. The single-ion anisotropy in the LTO and LTT phases of La_2NiO_4 are derived in Sec. IV. In Sec. V, we calculate the spin-wave spectra for the derived effective spin Hamiltonians. The origin of the weak ferromagnetism in cuprates and nickelates is also discussed. Conclusions are given in Sec. VI.

II. SUPEREXCHANGE INTERACTIONS

In this section we derive the superexchange interaction in the NiO_2 and CuO_2 planes by the perturbation theory. The Ni ion has two holes in the $3d$ orbitals, $x'^2-y'^2$ and $3z'^2-r'^2$, in the NiO_6 octahedron (see Fig. 1). The Hamiltonian for the holes in the NiO_2 plane is written by taking into account the spin-orbit coupling as follows:

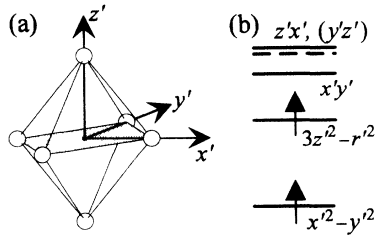

FIG. 1. (a) The NiO_6 octahedron and the $x'y'z'$-coordinate system. Open circles indicate O ions forming the octahedron; the Ni ion is located at the center. The shaded area is a section of the NiO_2 plane. (b) The crystal-field-level structure in the $x'y'z'$-coordinate system. Two holes are indicated by arrows.

$$H=H_0+H_t+H_{LS} , \tag{1}$$

with

$$\begin{aligned} H_0&=\sum_{jm\sigma}\varepsilon_m d^\dagger_{jm\sigma}d_{jm\sigma}+\sum_{kn\sigma}\varepsilon_{p_n}p^\dagger_{kn\sigma}p_{kn\sigma} \\ &\quad+\sum_{jmm'}U_{mm'}n_{jm}n_{jm'} , \\ H_t&=\sum_{jm\sigma}\sum_{k(j)n\sigma}(t_{jm,kn}d^\dagger_{jm\sigma}p_{kn\sigma}+\text{H.c.}) , \end{aligned} \tag{2}$$

and

$$H_{LS}=\lambda\sum_j(\mathbf{L}^{\mathrm{I}}_j\cdot\mathbf{S}^{\mathrm{I}}_j+\mathbf{L}^{\mathrm{II}}_j\cdot\mathbf{S}^{\mathrm{II}}_j) , \tag{3}$$

where $k(j)$ denotes the kth O site of the neighboring Ni site j, $d^\dagger_{jm\sigma}$ is the creation operator of a hole with spin σ on the mth $3d$ orbital of the jth Ni ion, ε_m is the crystal-field level of the mth $3d$ orbital, $p^\dagger_{kn\sigma}$ is the creation operator of a hole with spin σ on the kth $2p_n$ orbital ($n=x$, y, and z) of the jth O ion, ε_{p_n} is the energy of the kth $2p_n$ orbital, and n_{jm} is the number operator for the hole on the mth $3d$ orbital of the jth Ni ion. The energies are measured from the lowest energy level of the Ni $3d$ orbitals. $U_{mm'}$ is the Coulomb interaction constant between holes on the Ni site. $t_{jm,kn}$ denotes the transfer of a hole between the mth orbital of the Ni ion j and one of the $2p_n$ orbitals of the neighboring O ions k; a number of nonzero $t_{jm,kn}$ appear due to lattice distortions. $\mathbf{L}^{\mathrm{I}}_j$ and $\mathbf{L}^{\mathrm{II}}_j$ denote the orbital angular momenta with magnitude 2 at the j site. $\mathbf{S}^{\mathrm{I}}_j$ and $\mathbf{S}^{\mathrm{II}}_j$ denote the operators of spin $\frac{1}{2}$ at the j site. I and II are the superscripts for two holes on a Ni ion. λ is the spin-orbit coupling constant.

Let us apply the perturbation theory. In the first order of λ, we obtain the following Hamiltonian:

$$\begin{aligned} H&=\sum_{kn\sigma}\varepsilon_{p_n}p^\dagger_{kn\sigma}p_{kn\sigma}+U_{01}\sum_j n_{j0}n_{j1}+U\sum_j d^\dagger_{j0\uparrow}d^\dagger_{j0\downarrow}d_{j0\downarrow}d_{j0\uparrow}+U\sum_j d^\dagger_{j1\uparrow}d^\dagger_{j1\downarrow}d_{j1\downarrow}d_{j1\uparrow} \\ &\quad+\sum_{jk(j)n}\sum_\sigma(t_{j0,kn}d^\dagger_{j0\sigma}p_{kn\sigma}+\text{H.c.})+\sum_{jk(j)n}\sum_{\alpha\beta}[\mathbf{C}_{j0,kn}\cdot(d^\dagger_{j0\alpha}\boldsymbol{\sigma}_{\alpha\beta}p_{kn\beta})+\text{H.c.}] \\ &\quad+\sum_{jk(j)n}\sum_\sigma(t_{j1,kn}d^\dagger_{j1\sigma}p_{kn\sigma}+\text{H.c.})+\sum_{jk(j)n}\sum_{\alpha\beta}[\mathbf{C}_{j1,kn}\cdot(d^\dagger_{j1\alpha}\boldsymbol{\sigma}_{\alpha\beta}p_{kn\beta})+\text{H.c.}] , \end{aligned} \tag{4}$$

with

$$\mathbf{C}_{j0,kn}=-\frac{\lambda}{2}\sum_m \frac{\mathbf{L}^*_{jm0}}{\varepsilon_m}t_{jm,kn}\ ,$$
$$\mathbf{C}_{j1,kn}=-\frac{\lambda}{2}\sum_m \frac{\mathbf{L}^*_{jm1}}{\varepsilon_m}t_{jm,kn}\ , \tag{5}$$

where $\sigma_{\alpha\beta}$ is the Pauli spin matrix, 0 and 1 denote $x'^2-y'^2$ and $3z'^2-r^2$ orbital of the jth Ni ion, respectively, and $\mathbf{L}^*_{jm0}(\mathbf{L}^*_{jm1})$ is the complex conjugate of the matrix element of $\mathbf{L}_j$ between the mth and the ground (first-excited) state orbital of the jth Ni ion. We assume that $U_{mm'}$ is independent of mm' by writing U, but we retain the subscripts in the second term of Eq. (4) as $U_{01}(=U)$ for convenience. By examining the fourth-order terms with respect to the transfer parameters t and $\mathbf{C}$ in Eq. (4), we find the superexchange interaction between the spins on the Ni ions:

$$H=\sum_{\langle ij\rangle pq} J^{pq}\mathbf{S}^p_i\cdot\mathbf{S}^q_j+\sum_{\langle ij\rangle pq}\mathbf{D}^{pq}_{ij}\cdot(\mathbf{S}^p_i\times\mathbf{S}^q_j)+\sum_{\langle ij\rangle pq}\mathbf{S}^p_i\overleftrightarrow{\Gamma}^{pq}_{ij}\mathbf{S}^q_j\ , \tag{6}$$

with

$$J^{pq}=4\sum_{nn'}(t_{ip,kn}t_{kn,jq}+\mathbf{C}_{ip,kn}\cdot\mathbf{C}_{kn,jq})g_{nn'}(t_{jq,kn'}t_{kn',ip}+\mathbf{C}_{jq,kn'}\cdot\mathbf{C}_{kn',ip})\ , \tag{7}$$

$$\mathbf{D}^{pq}_{ij}=-4i\sum_{nn'}[(\mathbf{C}_{ip,kn}t_{kn,jq}+t_{ip,kn}\cdot\mathbf{C}_{kn,jq})g_{nn'}(t_{jq,kn'}t_{kn',ip}+\mathbf{C}_{jq,kn'}\cdot\mathbf{C}_{kn',ip})$$
$$-(t_{ip,kn}t_{kn,jq}+\mathbf{C}_{ip,kn}\cdot\mathbf{C}_{kn,jq})g_{nn'}(\mathbf{C}_{jq,kn'}t_{kn',ip}+t_{jq,kn'}\cdot\mathbf{C}_{kn',ip})]\ , \tag{8}$$

and

$$\overleftrightarrow{\Gamma}^{pq}_{ij}=4\sum_{nn'}\{(\overleftarrow{\mathbf{C}}_{ip,kn}t_{kn,jq}+t_{ip,kn}\cdot\overleftarrow{\mathbf{C}}_{kn,jq})g_{nn'}(\overrightarrow{\mathbf{C}}_{jq,kn'}t_{kn',ip}+t_{jq,kn'}\cdot\overrightarrow{\mathbf{C}}_{kn',ip})$$
$$+(\overleftarrow{\mathbf{C}}_{jq,kn}t_{kn,ip}+t_{jq,kn}\cdot\overleftarrow{\mathbf{C}}_{kn,ip})g_{nn'}(\overrightarrow{\mathbf{C}}_{ip,kn'}t_{kn',jq}+t_{ip,kn'}\cdot\overrightarrow{\mathbf{C}}_{kn',jq})$$
$$-\overleftrightarrow{1}[(\mathbf{C}_{ip,kn}t_{kn,jq}+t_{ip,kn}\cdot\mathbf{C}_{kn,jq})g_{nn'}(\mathbf{C}_{jq,kn'}t_{kn',ip}+t_{jq,kn'}\cdot\mathbf{C}_{kn',ip})]\}\ , \tag{9}$$

where p and q denote 0 or 1. The vector with the arrow $\leftarrow$ or $\rightarrow$ indicates that the inner product is taken with the spin operator put in the direction of the arrow. $\overleftrightarrow{1}$ is a 3×3 unit matrix. $g_{nn'}$ is given by

$$g_{nn'}=\begin{cases}\dfrac{1}{(\varepsilon_{p_n}-U_{01})^2}\left[\dfrac{1}{U}+\dfrac{1}{(\varepsilon_{p_n}-U_{01})}\right] & (n=n')\\ \dfrac{1}{(\varepsilon_{p_n}-U_{01})(\varepsilon_{p_{n'}}-U_{01})}\dfrac{1}{U}+\dfrac{1}{2}\left[\dfrac{1}{(\varepsilon_{p_n}-U_{01})}+\dfrac{1}{(\varepsilon_{p_{n'}}-U_{01})}\right]^2\dfrac{1}{\varepsilon_{p_n}+\varepsilon_{p_{n'}}-2U_{01}} & (n\neq n')\ .\end{cases} \tag{10}$$

The two 1/2 spins in the Ni ion form a spin 1 because of the Hund coupling. By restricting the magnitude of the spin on the Ni ion to be 1, the effective superexchange interaction between the neighboring spins on the Ni ion is derived from Eq. (6) as follows:

$$H=J\sum_{\langle ij\rangle}\mathbf{S}_i\cdot\mathbf{S}_j+\sum_{\langle ij\rangle}\mathbf{D}_{ij}\cdot(\mathbf{S}_i\times\mathbf{S}_j)+\sum_{\langle ij\rangle}\mathbf{S}_i\overleftrightarrow{\Gamma}_{ij}\mathbf{S}_j\ , \tag{11}$$

with

$$J=\frac{1}{4}(J^{00}+J^{10}+J^{01}+J^{11})\ , \tag{12}$$

$$\mathbf{D}_{ij}=\tfrac{1}{4}(\mathbf{D}^{00}_{ij}+\mathbf{D}^{10}_{ij}+\mathbf{D}^{01}_{ij}+\mathbf{D}^{11}_{ij})\ , \tag{13}$$

and

$$\overleftrightarrow{\Gamma}_{ij}=\tfrac{1}{4}(\overleftrightarrow{\Gamma}^{00}_{ij}+\overleftrightarrow{\Gamma}^{10}_{ij}+\overleftrightarrow{\Gamma}^{01}_{ij}+\overleftrightarrow{\Gamma}^{11}_{ij})\ . \tag{14}$$

If one eliminates the terms involving $\mathbf{S}^1_i$ and $\mathbf{S}^1_j$ in Eq. (6) and puts U_{01} to be zero in Eq. (10), one obtains the expression of the superexchange interaction for the CuO_2 plane:[20]

$$H=J\sum_{\langle ij\rangle}\mathbf{S}_i\cdot\mathbf{S}_j+\sum_{\langle ij\rangle}\mathbf{D}_{ij}\cdot(\mathbf{S}_i\times\mathbf{S}_j)+\sum_{\langle ij\rangle}\mathbf{S}_i\overleftrightarrow{\Gamma}_{ij}\mathbf{S}_j\ , \tag{15}$$

with

$$J=J^{00}\ , \tag{16}$$

$$\mathbf{D}_{ij}=\mathbf{D}^{00}_{ij}\ , \tag{17}$$

and

$$\overleftrightarrow{\Gamma}_{ij}=\overleftrightarrow{\Gamma}^{00}_{ij}\ . \tag{18}$$

Now let us consider the transfer parameters t and $\mathbf{C}$, and determine the expressions of the superexchange interactions in Eqs. (11) and (15). The crystal structures of the LTO and LTT phases are illustrated in Fig. 2. In the LTO phase, the octahedra involving $3d$ magnetic ion rotate alternately about the a axis, and in the LTT phase,

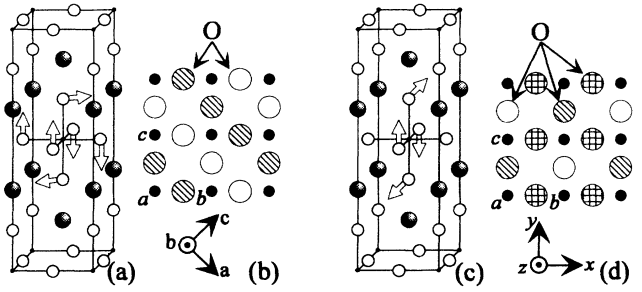

FIG. 2. (a) La_2CuO_4-type crystal structure in the LTO phase. The open arrows indicate the tilting of the octahedron. (b) The MO_2 (M = Cu, Ni) plane of the LTO phase: the O ions indicated by an open (hatched) circle are tilted up (down) out of the plane. (c) As in (a), but for the LTT phase. (c) As in (b), but for the LTT phase. The checked circles indicate the O ions remain in the plane.

the octahedra rotate alternately about the x axis. The coordination of ligand ions is responsible for the crystal-field level structure. The $3d$ crystal-field orbitals are represented as $x'^2-y'^2$, $3z'^2-r^2$, $x'y'$, $y'z'$, and $z'x'$ with respect to $x'y'z'$-coordinate system shown in Fig. 1. These orbitals may be written in the xyz-coordinate system by

$$
\begin{aligned}
&|x'^2-y'^2\rangle=|x^2-y^2\rangle+\frac{\delta}{\sqrt{2}}(|yz\rangle-|zx\rangle)\ ,\\
&|3z'^2-r'^2\rangle=|3z^2-r^2\rangle+\delta\sqrt{\tfrac{3}{2}}(|yz\rangle+|zx\rangle)\ ,\\
&|y'z'\rangle=|yz\rangle-\frac{\delta}{\sqrt{2}}(|x^2-y^2\rangle+\sqrt{3}|3z^2-r^2\rangle-|xy\rangle)\ ,\\
&|z'x'\rangle=|zx\rangle-\frac{\delta}{\sqrt{2}}(-|x^2-y^2\rangle+\sqrt{3}|3z^2-r^2\rangle-|xy\rangle)\ ,\\
&|x'y'\rangle=|xy\rangle-\frac{\delta}{\sqrt{2}}(|yz\rangle+|zx\rangle)\ ,
\end{aligned}
\tag{19}
$$

in the LTO phase, and by

$$
\begin{aligned}
&|x'^2-y'^2\rangle=|x^2-y^2\rangle+\delta|yz\rangle\ ,\\
&|3z'^2-r'^2\rangle=|3z^2-r^2\rangle+\delta\sqrt{3}|yz\rangle\ ,\\
&|y'z'\rangle=|yz\rangle-\delta(|x^2-y^2\rangle+\sqrt{3}|3z^2-r^2\rangle)\ ,\\
&|z'x'\rangle=|zx\rangle+\delta|xy\rangle\ ,\\
&|x'y'\rangle=|xy\rangle-\delta|zx\rangle\ ,
\end{aligned}
\tag{20}
$$

in the LTT phase, where δ is the tilting angle of the octahedron. These expressions are used to obtain $\mathbf{L}^*_{jm0}$ and $\mathbf{L}^*_{jm1}$ in the expression of $\mathbf{C}$'s. The representation of the $2p$ orbitals in the tilting $x'y'z'$-coordinate system is useful for obtaining $t_{jm,kn}$; they are given by

$$
\begin{aligned}
&|p_x\rangle=|p_{x'}\rangle+\frac{\delta}{\sqrt{2}}|p_{z'}\rangle\ ,\\
&|p_z\rangle=|p_{z'}\rangle-\frac{\delta}{\sqrt{2}}(|p_{x'}\rangle-|p_{y'}\rangle)\ ,\\
&|p_y\rangle=|p_{y'}\rangle-\frac{\delta}{\sqrt{2}}|p_{z'}\rangle\ ,
\end{aligned}
\tag{21}
$$

in the LTO phase, and by

$$
\begin{aligned}
&|p_x\rangle=|p_{x'}\rangle\ ,\\
&|p_z\rangle=|p_{z'}\rangle-\delta|p_{y'}\rangle\ ,\\
&|p_y\rangle=|p_{y'}\rangle+\delta|p_{z'}\rangle\ ,
\end{aligned}
\tag{22}
$$

in the LTT phase. Inserting the orbitals of Eqs. (19) and (21) into Eq. (8), we have the expressions for the $\mathbf{D}^{pq}_{ab}$ and $\mathbf{D}^{pq}_{ac}$ in the LTO phase as

$$
\begin{aligned}
&\mathbf{D}^{pq}_{ab}=(0,d^{pq}_{\mathrm{LTO}},0)\ ,\\
&\mathbf{D}^{pq}_{ac}=(-d^{pq}_{\mathrm{LTO}},0,0)\ ,
\end{aligned}
\tag{23}
$$

with

$$
\begin{aligned}
d^{pq}_{\mathrm{LTO}}=T^{pq}\times\Bigg\{&\frac{1}{(\varepsilon_{p_\sigma}-U_{01})^2}\left[\frac{1}{U}+\frac{1}{(\varepsilon_{p_\sigma}-U_{01})}\right]\\
&+\frac{1}{U}\frac{1}{(\varepsilon_{p_\sigma}-U_{01})(\varepsilon_{p_z}-U_{01})}\\
&+\frac{1}{2}\left[\frac{1}{(\varepsilon_{p_\sigma}-U_{01})}+\frac{1}{(\varepsilon_{p_z}-U_{01})}\right]^2\\
&\times\frac{1}{\varepsilon_{p_\sigma}+\varepsilon_{p_z}-2U_{01}}\Bigg\}\ ,
\end{aligned}
\tag{24}
$$

where

$$
\begin{aligned}
&T^{00}=-\lambda\delta\frac{4\sqrt{2}}{\varepsilon_{zx}}t_{zx,p_z}(t_{x^2-y^2})^3\ ,\\
&T^{11}=\sqrt{3}\lambda\delta\frac{4\sqrt{2}}{\varepsilon_{zx}}t_{zx,p_z}(t_{3z^2-r^2})^3\ ,\\
&T^{10}=T^{01}\\
&\quad=\frac{1}{2}\left[\sqrt{3}\lambda\delta\frac{4\sqrt{2}}{\varepsilon_{zx}}t_{zx,p_z}t_{3z^2-r^2}(t_{x^2-y^2})^2\right.\\
&\qquad\left.-\lambda\delta\frac{4\sqrt{2}}{\varepsilon_{zx}}t_{zx,p_z}t_{x^2-y^2}(t_{3z^2-r^2})^2\right]\ .
\end{aligned}
\tag{25}
$$

Here we have used $\varepsilon_{yz}=\varepsilon_{zx}$. ε_{p_σ} is the energy of the $2p_\sigma$ orbital, and t_{zx,p_z} is the transfer parameter of a hole between the $3d_{zx}$ and O $2p_z$ orbitals. $t_{x^2-y^2}(t_{3z^2-r^2})$ is the transfer between $3d_{x^2-y^2}$ ($3d_{3z^2-r^2}$) and O $2p_\sigma$ orbitals. By inserting the orbitals of Eqs. (20) and (22) into Eq. (8), we have

$$
\begin{aligned}
&\mathbf{D}^{pq}_{ab}=(0,0,0)\ ,\\
&\mathbf{D}^{pq}_{ac}=(-\sqrt{2}d^{pq}_{\mathrm{LTO}},0,0)\ ,
\end{aligned}
\tag{26}
$$

in the LTT phase. The schematic representation of the spatial pattern of the DM interaction of the LTO and LTT phases is shown in Fig. 3.

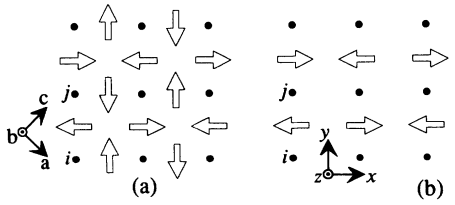

FIG. 3. The spatial pattern of the DM vectors $\mathbf{D}_{ij}$ (indicated by the open arrows) of (a) the LTO phase and (b) LTT phase. The arrows for the DM vectors are drawn by noting that the site j is always in the right or upper direction of the site i.

III. ANISOTROPIC-EXCHANGE INTERACTIONS FROM DIRECT-EXCHANGE MECHANISM

In the previous section, we have derived the DM and pseudodipolar interactions by considering the superexchange mechanisms; the DM interaction is linear in the spin-orbit coupling constant λ and also in the tilting angle δ of the octahedron, and the pseudodipolar interaction is of the second order of both λ and δ. Evaluating the parameter values as $\lambda \sim 0.1$ eV,[21] $\delta \sim 0.05$ rad [for the LTO phase of La_2CuO_4 (Ref. 22)], and $\varepsilon_{yz} \sim 1$ eV,[23] we find that the magnitude of the pseudodipolar interaction is roughly $\delta^2(\lambda/\varepsilon)^2 J \sim 10^{-5} J$. The pseudodipolar interaction with direct-exchange mechanism thus cannot be neglected. Shekhtman, Aharony, and Entin-Wohlman[16,19] first pointed out the importance of the direct-exchange pseudodipolar interaction in the magnetism of the cuprates. The anisotropic-exchange interactions of direct-exchange mechanism is given, e.g., by the following perturbation process (see Fig. 4); (i) the spin on the x^2-y^2 orbital at i site goes to the zx orbital at the same magnetic ion by using the spin-orbit coupling, (ii) the direct-exchange interaction acts between the spin on the zx orbital at i site and the spin on the x^2-y^2 orbital at j site, and (iii) the spin on the zx orbital at i site returns to the x^2-y^2 orbital at the same magnetic ion by using the spin-orbit coupling. We thus obtain the direct-exchange pseudodipolar interaction

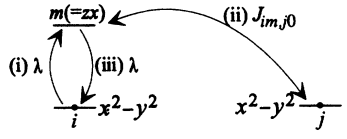

FIG. 4. One of the perturbation processes for the anisotropic-exchange interactions of direct-exchange mechanism.

$$H^d = \sum_{\langle ij \rangle} \mathbf{S}_i \overleftrightarrow{\Gamma}^d_{ij} \mathbf{S}_j \ , \tag{27}$$

where $\overleftrightarrow{\Gamma}^d_{ij}$ is given by

$$\overleftrightarrow{\Gamma}^d_{ij} = \frac{1}{4} \sum_{pq} \overleftrightarrow{\Gamma}^d_{ip,jq} \tag{28}$$

for nickelates and by

$$\overleftrightarrow{\Gamma}^d_{ij} = \overleftrightarrow{\Gamma}^d_{i0,j0} \tag{29}$$

for cuprates. We find

$$\overleftrightarrow{\Gamma}^d_{ip,jq} = \lambda^2 \frac{1}{4} \left\{ \sum_m \frac{J_{im,jq}}{(\varepsilon_m - \varepsilon_p)^2} [\overleftarrow{\mathbf{L}}_{ipm} \vec{\mathbf{L}}_{imp} + \overleftarrow{\mathbf{L}}_{imp} \vec{\mathbf{L}}_{ipm} - \overleftrightarrow{1}(\mathbf{L}_{ipm} \cdot \mathbf{L}_{imp})] \right.$$
$$\left. \times \sum_m \frac{J_{ip,jm}}{(\varepsilon_m - \varepsilon_q)^2} [\overleftarrow{\mathbf{L}}_{jqm} \vec{\mathbf{L}}_{jmq} + \overleftarrow{\mathbf{L}}_{jmq} \vec{\mathbf{L}}_{jqm} - \overleftrightarrow{1}(\mathbf{L}_{jqm} \cdot \mathbf{L}_{jmq})] \right\} , \tag{30}$$

where $J_{im,jq}$ is the direct-exchange interaction between spins on the mth orbital at i site and the qth orbital at j site. The direct-exchange pseudodipolar interaction does not require the lattice distortion; the effect of the lattice distortion can be neglected. This is in contrast to the superexchange pseudodipolar interaction for which the lattice distortion is essential. We obtain the structure of the direct-exchange pseudodipolar interaction by considering the coordinations of the $3d$ orbitals and $2p$ orbitals:

$$\mathbf{S}_a \overleftrightarrow{\Gamma}_{ab} \mathbf{S}_b = (S^x_a \ S^y_a \ S^z_a) \times \begin{bmatrix} -(\Gamma_1+\Gamma_2) & 0 & 0 \\ 0 & \Gamma_1-\Gamma_2 & 0 \\ 0 & 0 & \Gamma_2-\Gamma_1 \end{bmatrix} \begin{bmatrix} S^x_b \\ S^y_b \\ S^z_b \end{bmatrix} , \tag{31}$$

$$\mathbf{S}_a \overleftrightarrow{\Gamma}_{ac} \mathbf{S}_c = (S^x_a \ S^y_a \ S^z_a) \times \begin{bmatrix} \Gamma_1-\Gamma_2 & 0 & 0 \\ 0 & -(\Gamma_1+\Gamma_2) & 0 \\ 0 & 0 & \Gamma_2-\Gamma_1 \end{bmatrix} \begin{bmatrix} S^x_c \\ S^y_c \\ S^z_c \end{bmatrix} ,$$

where

$$\Gamma_1 = \frac{\lambda^2}{2} \left[\frac{J_{azx,b0}}{2(\varepsilon_{zx})^2} + \frac{J_{azx,b1}}{2(\varepsilon_{zx}-\varepsilon_1)^2} \right] ,$$
$$\Gamma_2 = \frac{\lambda^2}{2} \left[\frac{2J_{axy,b0}}{(\varepsilon_{xy})^2} + \frac{2J_{axy,b1}}{(\varepsilon_{xy}-\varepsilon_1)^2} \right] , \tag{32}$$

for nickelates and

$$\Gamma_1=\lambda^2\frac{J_{azx,b0}}{2(\varepsilon_{zx})^2}\ ,$$
$$\Gamma_2=\lambda^2\frac{2J_{axy,b0}}{(\varepsilon_{xy})^2}\ , \tag{33}$$

for cuprates. Here we have used the relations $\varepsilon_{zx}=\varepsilon_{yz}$ and $J_{im,jq}=J_{iq,jm}$. By using $\varepsilon_{zx}>\varepsilon_{xy}>\varepsilon_1$,[23] $J_{azx,b0}=J_{axy,b0}(<0)$, and $J_{azx,b1}=J_{axy,b1}(<0)$, we obtain $\Gamma_1>\Gamma_2$. $\overleftrightarrow{\Gamma}_{ab}$ and $\overleftrightarrow{\Gamma}_{ac}$ provide the anisotropy along the bonds a-b and a-c, respectively. As a result, the direct-exchange pseudodipolar interactions compete with each other. Because of this competition, the in-plane anisotropy of the direct-exchange pseudodipolar interaction vanishes, and only the easy-plane anisotropy remains.

IV. SINGLE-ION ANISOTROPY

Single-ion anisotropy exists in the nickelates since the Ni spin is 1. The expression for the single-ion anisotropy is well known and is written as

$$H_A=-\sum_{\mu\nu}A_{\mu\nu}S^\mu S^\nu\ , \tag{34}$$

with

$$A_{\mu\nu}=\left[\frac{\lambda}{2}\right]^2\sum_m\frac{(L_\mu^{\rm I}+L_\mu^{\rm II})_{0m}(L_\nu^{\rm I}+L_\nu^{\rm II})_{m0}}{\varepsilon_m}\ . \tag{35}$$

The structure of the single-ion anisotropy is determined by the structure of the crystal-field levels characterized by the symmetry of the NiO_6 octahedron reduced by the lattice distortion. The observed[5] symmetry of the NiO_6 octahedron is illustrated in Fig. 5 for the LTO and the LTT phases. The degenerate crystal-field levels for the $y'z'$ and $z'x'$ orbitals split into two nondegenerate levels. These orbitals are represented as $c'b'$ and $a'b'$ with respect to the tilting $a'b'c'$ coordinate in the LTO phase, and as $y'z'$ and $z'x'$ with respect to the tilting $x'y'z'$ coordinate in the LTT phase. We thus obtain the expressions for the single-ion anisotropy

$$A^{c'c'}=\left[\frac{\lambda}{2}\right]^2\left[\frac{1}{\varepsilon_{c'b'}}+\frac{3}{\varepsilon_{a'b'}-\varepsilon_{3z'^2-r'^2}}\right]\ ,$$
$$A^{a'a'}=\left[\frac{\lambda}{2}\right]^2\left[\frac{1}{\varepsilon_{a'b'}}+\frac{3}{\varepsilon_{c'b'}-\varepsilon_{3z'^2-r'^2}}\right]\ , \tag{36}$$
$$A^{b'b'}=\left[\frac{\lambda}{2}\right]^2\left[\frac{4}{\varepsilon_{x'y'}}\right]\ ,$$

for the LTO phase by using $a'b'c'$ coordinates, and

$$A^{x'x'}=\left[\frac{\lambda}{2}\right]^2\left[\frac{1}{\varepsilon_{y'z'}}+\frac{3}{\varepsilon_{y'z'}-\varepsilon_{3z'^2-r'^2}}\right]\ ,$$
$$A^{y'y'}=\left[\frac{\lambda}{2}\right]^2\left[\frac{1}{\varepsilon_{z'x'}}+\frac{3}{\varepsilon_{z'x'}-\varepsilon_{3z'^2-r'^2}}\right]\ , \tag{37}$$
$$A^{z'z'}=\left[\frac{\lambda}{2}\right]^2\left[\frac{4}{\varepsilon_{x'y'}}\right]\ ,$$

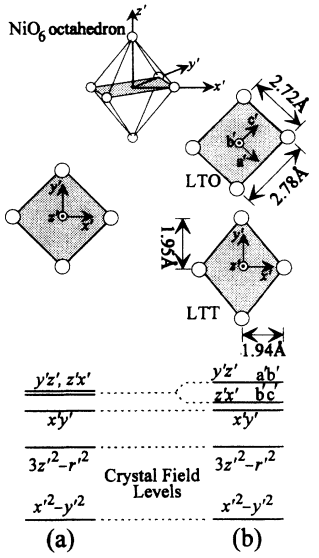

FIG. 5. Distortions of the NiO_6 octahedron in the LTO and LTT phases (Ref. 5), and changes in the crystal-field levels due to symmetry reduction. (a) The crystal-field-level structure for the undistorted NiO_6 octahedron: the $z'x'$ and $y'z'$ levels are degenerate because the cross section in the $x'y'$ plane is square for the octahedron with the D_{4h}-group symmetry. (b) The crystal-field-level structure for the distorted NiO_6 octahedron in the LTO and LTT phases: the degeneracy between the $z'x'$ and $y'z'$ levels is lifted because the octahedron has the D_{2h}-group symmetry where the crossection in the $x'y'$ plane is rectangular in the LTO phase and diamonds in the LTT phase.

for the LTT phase by using the $x'y'z'$ coordinates. In the LTO phase, the energy level of the $c'b'$ orbital is lower than the energy level of the $a'b'$ orbital because the O^{2-} ion approaches the electron cloud of the $c'b'$ orbital by the distortion of the NiO_6 octahedron. Then, we have

$$A^{a'a'}>A^{c'c'}>A^{b'b'}\ . \tag{38}$$

In the LTT phase, the energy level of the $y'z'$ orbital is higher than the energy level of the $z'x'$ orbital because the O^{2-} ion goes away from the electron cloud of the $y'z'$ orbital by the distortion of the NiO_6 octahedron. Then, we have

$$A^{y'y'}>A^{x'x'}>A^{z'z'}\ . \tag{39}$$

V. SPIN-WAVE THEORY

In this section we explore the spin-wave theory in the LTO and LTT phases of the cuprates and nickelates.

First let us consider the cuprates. The Cu ions have spin $\frac{1}{2}$, so that the single-ion anisotropy does not exist in the spin system. The spin Hamiltonian for the cuprates consists of the superexchange interaction Eq. (15) and direct-exchange interaction Eq. (27):

$$H=J\sum_{\langle ij\rangle}\mathbf{S}_i\cdot\mathbf{S}_j+\sum_{\langle ij\rangle}\mathbf{D}_{ij}\cdot(\mathbf{S}_i\times\mathbf{S}_j)+\sum_{\langle ij\rangle}\mathbf{S}_i\overleftrightarrow{\Gamma}_{ij}\mathbf{S}_j\ . \tag{40}$$

The structure of the DM and pseudodipolar interactions

obtained by the perturbation calculations are given, respectively, by

$$\mathbf{D}_{ab}=\frac{1}{\sqrt{2}}(-d,d,0)\ ,$$
$$\mathbf{D}_{ac}=\frac{1}{\sqrt{2}}(-d,-d,0)\ , \tag{41}$$

and

$$\overleftrightarrow{\Gamma}_{ab}=\begin{bmatrix} -\Gamma_2 & -\Gamma_1-\Gamma^S & 0 \\ -\Gamma_1-\Gamma^S & -\Gamma_2 & 0 \\ 0 & 0 & \Gamma_2-\Gamma_1-\Gamma^S \end{bmatrix},$$
$$\overleftrightarrow{\Gamma}_{ac}=\begin{bmatrix} -\Gamma_2 & \Gamma_1+\Gamma^S & 0 \\ \Gamma_1+\Gamma^S & -\Gamma_2 & 0 \\ 0 & 0 & \Gamma_2-\Gamma_1-\Gamma^S \end{bmatrix}, \tag{42}$$

with respect to the *acb* coordinate in the LTO phase and by

$$\mathbf{D}_{ab}=(0,0,0)\ ,$$
$$\mathbf{D}_{ac}=(-d,0,0)\ , \tag{43}$$

and

$$\overleftrightarrow{\Gamma}_{ab}=\begin{bmatrix} -(\Gamma_1+\Gamma_2) & 0 & 0 \\ 0 & \Gamma_1-\Gamma_2 & 0 \\ 0 & 0 & \Gamma_2-\Gamma_1 \end{bmatrix},$$
$$\overleftrightarrow{\Gamma}_{ac}=\begin{bmatrix} \Gamma_1+\Gamma_2+\Gamma^S & 0 & 0 \\ 0 & -\Gamma_1-\Gamma_2-\Gamma^S & 0 \\ 0 & 0 & \Gamma_2-\Gamma_1-\Gamma^S \end{bmatrix}, \tag{44}$$

with respect to the *xyz* coordinate in the LTT phase (see Fig. 3).

The spin-wave spectrum is calculated straightforwardly if one knows the classical ground state of the Hamiltonian. In the LTO phase, the classical ground state is readily calculated and determined uniquely as shown in Fig. 6(a). This system has the weak ferromagnetism, where the spin canting angle θ_{LTO} is given by

$$\theta_{\mathrm{LTO}}=\tfrac{1}{2}\tan^{-1}\frac{d/\sqrt{2}}{J-\frac{1}{2}(\Gamma_1+\Gamma^S)}\ . \tag{45}$$

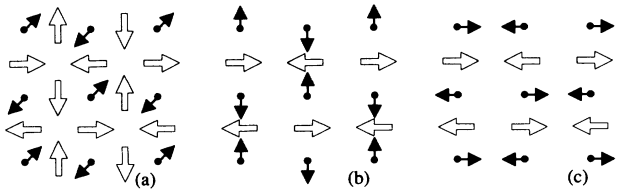

FIG. 6. The schematic representation of the spin structure (solid arrows) and direction of the DM vectors (open arrows) in the CuO_2 plane of the LTO and LTT phases. (a) The weak ferromagnetism in the LTO phase. All the spins cant up out of the plane. (b) The weak ferromagnetism in the LTT phase. All the spins cant up out of the plane. (c) The antiferromagnetism without spin canting in the LTT phase.

In the LTT phase, there are two possibilities of the spin structure in the classical system: one is the weak ferromagnetism with spin canting angle

$$\theta_{\mathrm{LTT}}=\tfrac{1}{2}\tan^{-1}\frac{d/2}{J-\frac{1}{2}(\Gamma_1+\Gamma^S)}\ , \tag{46}$$

and the other is the antiferromagnetism without spin canting [see Figs. 6(b) and 6(c)]. The classical ground-state energy of the weak-ferromagnetic spin arrangement [Fig. 6(b)] is given by $J+d^2/(8J)-\Gamma_2-\Gamma^S/2$ per plaquette, and that of antiferromagnetic spin arrangement without spin canting [Fig. 6(c)] is given by $J-\Gamma_2+\Gamma^S/2$ per plaquette. Thus, either the weak ferromagnetism or the antiferromagnetism without spin canting is realized depending on the sign of

$$\frac{d^2}{8J}-\Gamma^S\ . \tag{47}$$

Equation (47) represents a competition between the DM interaction d and the pseudodipolar interaction Γ^S. If the DM interaction wins so that Eq. (47) has a positive sign, weak ferromagnetism shown in Fig. 6(b) is realized, and if the DM interaction loses so that Eq. (47) has a negative sign, antiferromagnetism without spin canting shown in Fig. 6(c) is realized.

The deviations of spins from the classical spin structures correspond to the spin-wave excitation. Using the Holstein-Primakoff transformation, the deviations are represented by bosons and the spin-wave spectrum is obtained by a diagonalization of the spin Hamiltonian with respect to the bosons. This procedure gives the spectra with in-plane ($\varepsilon_i(\mathbf{k})$) and out-of-plane ($\varepsilon_o(\mathbf{k})$) modes: in the LTO phase we have

$$\varepsilon_i(\mathbf{k})=zS\sqrt{[J_2+\tfrac{1}{2}(J_3-J_1)\gamma_{\mathbf{k}}]^2-[\tfrac{1}{4}(J_3+J_1)^2\gamma_{\mathbf{k}}^2+J_4{}^2\gamma_{\mathbf{k}}'^2]}\ ,$$
$$\varepsilon_o(\mathbf{k})=zS\sqrt{[J_2-\tfrac{1}{2}(J_3-J_1)\gamma_{\mathbf{k}}]^2-[\tfrac{1}{4}(J_3+J_1)^2\gamma_{\mathbf{k}}^2+J_4{}^2\gamma_{\mathbf{k}}'^2]}\ , \tag{48}$$

with $z=4$ and $S=\frac{1}{2}$, where

$$
\begin{aligned}
&J_1=J-\Gamma_2\\
&J_2=\tfrac{1}{2}(\Gamma_1+\Gamma^S)-\Gamma_2+\sqrt{(d^2/2)+[J-\tfrac{1}{2}(\Gamma_1+\Gamma^S)]^2}\\
&J_3=\Gamma_2-\tfrac{1}{2}(\Gamma_1+\Gamma^S)+\sqrt{(d^2/2)+[J-\tfrac{1}{2}(\Gamma_1+\Gamma^S)]^2}\\
&J_4=(\Gamma_1+\Gamma^S)\sin\theta_{\mathrm{LTO}}-\frac{d}{\sqrt{2}}\cos\theta_{\mathrm{LTO}}\\
&\gamma_{\mathbf{k}}=\frac{1}{2}(\cos k_x+\cos k_y)\\
&\gamma'_{\mathbf{k}}=\frac{1}{2}(\cos k_x-\cos k_y)\ .
\end{aligned}
\tag{49}
$$

The zone-center spin-wave gaps are given by

$$
\begin{aligned}
\varepsilon_i(\mathbf{0})&=zS\sqrt{(J_2+J_3)(J_2-J_1)}\\
&\approx zS\frac{d}{\sqrt{2}}\ ,\\
\varepsilon_o(\mathbf{0})&=zS\sqrt{(J_2+J_1)(J_2-J_3)}\\
&\approx zS\sqrt{2J[2(\tfrac{1}{2}\Gamma_1-\Gamma_2)+\Gamma^S]}\ .
\end{aligned}
\tag{50}
$$

In the LTT phase we have two possibilities: when the weak ferromagnetism [Fig. 6(b)] is obtained the spectra are given by

$$
\begin{aligned}
&\varepsilon_i(\mathbf{k})=zS\sqrt{\{J_2+\tfrac{1}{2}[(J_3-J_1)\gamma_{\mathbf{k}}+(J_7-J_5)\gamma'_{\mathbf{k}}]\}^2-\tfrac{1}{4}[(J_3+J_1)\gamma_{\mathbf{k}}+(J_7+J_5)\gamma'_{\mathbf{k}}]^2}\ ,\\
&\varepsilon_o(\mathbf{k})=zS\sqrt{\{J_2-\tfrac{1}{2}[(J_3-J_1)\gamma_{\mathbf{k}}+(J_7-J_5)\gamma'_{\mathbf{k}}]\}^2-\tfrac{1}{4}[(J_3+J_1)\gamma_{\mathbf{k}}+(J_7+J_5)\gamma'_{\mathbf{k}}]^2}\ ,
\end{aligned}
\tag{51}
$$

and when the antiferromagnetism without spin canting [Fig. 6(c)] is obtained the spectra are given by

$$
\begin{aligned}
\varepsilon_i(\mathbf{k})=zS(&\{J_1+\tfrac{1}{2}[(J_2-J_3)\gamma_{\mathbf{k}}+(J_6-J_7)\gamma'_{\mathbf{k}}]\}^2\\
&-\{\tfrac{1}{4}[(J_2+J_3)\gamma_{\mathbf{k}}+(J_6+J_7)\gamma'_{\mathbf{k}}]^2\\
&+J_4{}^2\gamma'^2_{\mathbf{k}}\})^{1/2}\ ,\\
\varepsilon_o(\mathbf{k})=zS(&\{J_1-\tfrac{1}{2}[(J_2-J_3)\gamma_{\mathbf{k}}+(J_6-J_7)\gamma'_{\mathbf{k}}]\}^2\\
&-\{\tfrac{1}{4}[(J_2+J_3)\gamma_{\mathbf{k}}+(J_6+J_7)\gamma'_{\mathbf{k}}]^2\\
&+J_4{}^2\gamma'^2_{\mathbf{k}}\})^{1/2}\ .
\end{aligned}
\tag{52}
$$

J's in Eqs. (51) and (52) are defined by

$$
\begin{aligned}
&J_1=J-\Gamma_2+\tfrac{1}{2}\Gamma^S\ ,\\
&J_2=\tfrac{1}{2}\Gamma_1-\Gamma_2+\sqrt{\tfrac{1}{4}d^2+[J-\tfrac{1}{2}(\Gamma_1+\Gamma^S)]^2}\ ,\\
&J_3=\Gamma_2-\tfrac{1}{2}\Gamma_1+\sqrt{\tfrac{1}{4}d^2+[J-\tfrac{1}{2}(\Gamma_1+\Gamma^S)]^2}\ ,\\
&J_4=\tfrac{1}{2}d\cos2\theta_{\mathrm{LTT}}-\tfrac{1}{2}(\Gamma_1+\Gamma^S)\sin2\theta_{\mathrm{LTT}}\ ,\\
&J_5=-(\Gamma_1+\tfrac{1}{2}\Gamma^S)\ ,\\
&J_6=\tfrac{1}{2}\Gamma^S\cos2\theta_{\mathrm{LTT}}+\tfrac{1}{2}d\sin2\theta_{\mathrm{LTT}}-\Gamma_1\cos^2\theta_{\mathrm{LTT}}\ ,\\
&J_7=\tfrac{1}{2}\Gamma^S\cos2\theta_{\mathrm{LTT}}+\tfrac{1}{2}d\sin2\theta_{\mathrm{LTT}}+\Gamma_1\sin^2\theta_{\mathrm{LTT}}\ .
\end{aligned}
\tag{53}
$$

The zone-center spin-wave gaps are given by

$$
\begin{aligned}
\varepsilon_i(\mathbf{0})&=zS\sqrt{(J_2+J_3)(J_2-J_1)}\\
&\approx zS\sqrt{2J[(d^2/8J)-\Gamma^S]}\ ,\\
\varepsilon_o(\mathbf{0})&=zS\sqrt{(J_2+J_1)(J_2-J_3)}\\
&\approx zS\sqrt{4J(\tfrac{1}{2}\Gamma_1-\Gamma_2)}\ ,
\end{aligned}
\tag{54}
$$

in the weak-ferromagnetic case and by

$$
\begin{aligned}
\varepsilon_i(\mathbf{0})&=zS\sqrt{(J_1+J_3)(J_1-J_2)}\\
&\approx zS\sqrt{2J(\Gamma^S-(d^2/8J))}\ ,\\
\varepsilon_o(\mathbf{0})&=zS\sqrt{(J_1+J_2)(J_1-J_3)}\\
&\approx zS\sqrt{2J[2(\tfrac{1}{2}\Gamma_1-\Gamma_2)+(\Gamma^S-(d^2/8J))]}\ ,
\end{aligned}
\tag{55}
$$

in the antiferromagnetic case. We find in Eqs. (50), (54), and (55) that the in-plane and out-of-plane gaps are given, respectively, by the anisotropic-exchange interactions of superexchange and direct-exchange mechanisms.

Shekhtman, Entin-Wohlman, and Aharony[16] have proposed the frustration mechanism for the emergence of weak ferromagnetism in the LTO phase of La_2CuO_4. They have also concluded that only by the frustration mechanism there is no possibility of the emergence of weak ferromagnetism in the LTT phase. This is represented by the negative sign of Eq. (47). However, several groups[7-9] have observed the weak ferromagnetism in the LTT phase of $La_{1.65}Nd_{0.35}CuO_4$, indicating that Eq. (47) is positive. According to the results in Sec. II, the value of Γ^S is about two times larger than the value of the first term of Eq. (47). Thus, in the fourth-order perturbation shown in Sec. II, Eq. (47) becomes negative.[20] If the value of d increases only by $\sim 50\%$, Eq. (47) becomes positive. This means that a small quantitative change in the value of the terms in Eq. (47) can give rise to qualitatively different magnetism. In such a situation, one should carefully take into account the higher-order perturbations. The extensions of the perturbation expansion, however, becomes too complicated: the evaluation of such a tiny value by the perturbation is

usually unreliable. Thus, one should rather rely on the experimental facts that Eq. (47) must be positive. Without the effect of the multiorbitals one cannot obtain the positive sign of Eq. (47). We therefore propose that the effect of the multiorbitals be the origin of the observed weak ferromagnetism in the LTT phase of $La_{1.65}Nd_{0.35}CuO_4$. The observed weak ferromagnetism in the LTO phase of La_2CuO_4 may also be due to this effect.

It has been observed in $La_{1.65}Nd_{0.35}CuO_4$ that the in-plane spin-wave gap increases sensitively at the structural phase transition from the LTO phase to low-temperature phase (*Pccn*), but the out-of-plane gap is little affected.[8] It is straightforward to understand this experimental result from Eqs. (50) and (54): the tilting of the CuO_6 octahedra characterizes the structural phase transition, and as shown in Sec. II and III, the anisotropic exchange interactions of superexchange mechanism, which depends on the tilting angle of the CuO_6 octahedra, is responsible for the in-plane gap, but the anisotropic-exchange interactions of direct-exchange mechanism, which depends on the tilting angle very little, is responsible for the out-of-plane gap.

It has been reported that the in-plane and out-of-plane spin-wave gaps are 2.3 and 5.0 meV,[8] respectively, in the LTO phase of La_2CuO_4. Using these values and Eq. (50), we can estimate the values of the anisotropic-exchange interactions as

$$d \sim 1.63 \text{ meV} \tag{56}$$

and

$$2(\tfrac{1}{2}\Gamma_1-\Gamma_2)+\Gamma^S \sim 0.024 \text{ meV} , \tag{57}$$

where we use $J=130$ meV.[24] In the LTT phase of $La_{1.65}Nd_{0.35}CuO_4$, it has been reported that the in-plane and out-of-plane spin-wave gaps are 4.5 and 6.0 meV, respectively.[8] We can estimate the values of the anisotropic-exchange interactions from Eq. (54):

$$\left[\frac{d^2}{8J}-\Gamma^S\right] \sim 0.019 \text{ meV} \tag{58}$$

and

$$(\tfrac{1}{2}\Gamma_1-\Gamma_2) \sim 0.017 \text{ meV} . \tag{59}$$

Thus, we find that the observed spin-wave gaps for the two modes in both LTO- and LTT-phase cuprates can be explained with reasonable choice of the parameter values.

Next we discuss the spin-wave theory in the nickelates. Because the Ni ion has spin 1, the spin Hamiltonian for the NiO_2 plane includes not only the superexchange interaction Eq. (11) and direct-exchange interaction Eq. (27), but also the single-ion anisotropy:

$$H=J\sum_{\langle ij\rangle}\mathbf{S}_i\cdot\mathbf{S}_j+\sum_{\langle ij\rangle}\mathbf{D}_{ij}\cdot(\mathbf{S}_i\times\mathbf{S}_j)+\sum_{\langle ij\rangle}\mathbf{S}_i\vec{\Gamma}_{ij}\mathbf{S}_j+H_A , \tag{60}$$

where

$$H_A=-\sum_{\mu'}A^{\mu'\mu'}\left[\sum_{i\in A}(S_i^{\mu'})^2+\sum_{j\in B}(S_j^{\mu'})^2\right] . \tag{61}$$

H_A is the single-ion anisotropy. μ' refers to the $a'b'c'$-coordinate system in the LTO phase or to the $x'y'z'$-coordinate system in the LTT phase. The DM and pseudodipolar interactions have the same structure as those for the CuO_2 plane [see Eqs. (41)–(44)]. The leading terms in the DM and pseudodipolar interactions given in Eqs. (13), (14), and (28) are $\mathbf{D}_{ij}^{00}$, $\vec{\Gamma}_{ij}^{00}$, and $\vec{\Gamma}_{i0,j0}^{d}$, which are of the same orders of magnitude as those for cuprates. The spin-wave gaps are observed in La_2NiO_4 to be 7.9 ± 0.6 meV (in-plane mode) and 16.2 ± 0.5 meV (out-of-plane mode) in the LTO phase, and 4.1 ± 0.4 meV (in-plane mode) and 15.7 ± 0.6 meV (out-of-plane mode) in the LTT phase.[10] These gaps cannot be explained by the exchange anisotropies, but can be explained by the single-ion anisotropy: the directions of the magnetic moment, or the magnetic structures observed in the LTO and the LTT phases, are consistent with those given by the structure of the single-ion anisotropy discussed in Sec. IV.

The classical magnetic structures of the Hamiltonian (60) in the LTO and LTT phases are shown in Fig. 7. In the LTO phase, the spins point to the direction of the a axis by the single-ion anisotropy; because in this direction the DM interaction of the LTO phase cannot provide weak ferromagnetism, the antiferromagnetism without spin canting is obtained. In the LTT phase, the spin system shows the weak ferromagnetism because the spins point to the direction of the y axis due to the single-ion anisotropy. The spin canting angle φ_{LTT} is given by

$$\varphi_{\mathrm{LTT}}=\tfrac{1}{2}\tan^{-1}\frac{z\frac{1}{2}d+(A^{yy}-A^{zz})\sin2\delta}{z[J-\frac{1}{2}(\Gamma_1+\Gamma^S)]+(A^{yy}-A^{zz})\cos2\delta} , \tag{62}$$

where d, Γ_1, and Γ^S are the exchange anisotropies between the spins of magnitude 1 on Ni ions, and δ is the tilting angle of the NiO_6 octahedron.

The spin-wave spectra with the in-plane and out-of-plane modes are derived straightforwardly: in the LTO phase we have

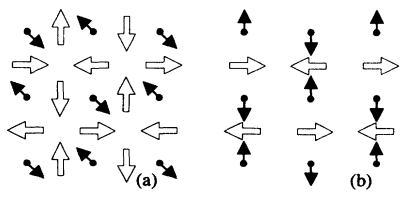

FIG. 7. The schematic representation of the spin structure (solid arrows) and direction of the DM vectors (open arrows) in the NiO_2 plane of the LTO and LTT phases. (a) The antiferromagnetism without spin canting in the LTO phase. (b) The weak ferromagnetism in the LTT phase where all the spins cant up out of the plane.

$$\varepsilon_i(\mathbf{k})=zS\left\{\left[J^{aa}+\frac{1}{z}[2A^{aa}-(A^{cc}-A^{bb})]-\tfrac{1}{2}(J^{cc}-J^{bb})\gamma_{\mathbf{k}}\right]^2 - \left[\left[\frac{1}{z}(A^{bb}-A^{cc})\cos 2\delta-\tfrac{1}{2}(J^{cc}+J^{bb})\gamma_{\mathbf{k}}\right]^2+\left[\frac{1}{z}(A^{bb}-A^{cc})\sin 2\delta-d\gamma_{\mathbf{k}}\right]^2\right]\right\}^{1/2} \tag{63}$$

$$\varepsilon_o(\mathbf{k})=zS\left\{\left[J^{aa}+\frac{1}{z}[2A^{aa}-(A^{cc}+A^{bb})]+\tfrac{1}{2}(J^{cc}-J^{bb})\gamma_{\mathbf{k}}\right]^2 - \left[\left[\frac{1}{z}(A^{bb}-A^{cc})\cos 2\delta+\tfrac{1}{2}(J^{cc}+J^{bb})\gamma_{\mathbf{k}}\right]^2+\left[\frac{1}{z}(A^{bb}-A^{cc})\sin 2\delta+d\gamma_{\mathbf{k}}\right]^2\right]\right\}^{1/2}, \tag{64}$$

where

$$J^{aa}=J^{cc}=J-\Gamma_2\,,\qquad J^{bb}=J+\Gamma_2-\Gamma_1-\Gamma^S\,, \tag{65}$$

and in the LTT phase we have

$$\varepsilon_i(\mathbf{k})=zS\left\{\left[J_2+\frac{1}{z}A^{yy}[2\cos^2(\delta-\theta)-\sin^2(\delta-\theta)]+\tfrac{1}{2}(J_3-J_1)\gamma_{\mathbf{k}} -\frac{1}{z}A^{xx}+\frac{1}{z}A^{zz}[2\sin^2(\delta-\theta)-\cos^2(\delta-\theta)]+\tfrac{1}{2}(J_5-J_4)\gamma'_{\mathbf{k}}\right]^2 - \left[\frac{1}{z}[A^{xx}-A^{zz}\cos^2(\delta-\theta)-A^{yy}\sin^2(\delta-\theta)]+\tfrac{1}{2}(J_3+J_1)\gamma_{\mathbf{k}}+\tfrac{1}{2}(J_5+J_4)\gamma'_{\mathbf{k}}\right]^2\right\}^{1/2}, \tag{66}$$

$$\varepsilon_o(\mathbf{k})=zS\left\{\left[J_2+\frac{1}{z}A^{yy}[2\cos^2(\delta-\theta)-\sin^2(\delta-\theta)]-\tfrac{1}{2}(J_3-J_1)\gamma_{\mathbf{k}} -\frac{1}{z}A^{xx}+\frac{1}{z}A^{zz}[2\sin^2(\delta-\theta)-\cos^2(\delta-\theta)]-\tfrac{1}{2}(J_5-J_4)\gamma'_{\mathbf{k}}\right]^2 - \left[\frac{1}{z}[A^{xx}-A^{zz}\cos^2(\delta-\theta)-A^{yy}\sin^2(\delta-\theta)]-\tfrac{1}{2}(J_3+J_1)\gamma_{\mathbf{k}}-\tfrac{1}{2}(J_5+J_4)\gamma'_{\mathbf{k}}\right]^2\right\}^{1/2}, \tag{67}$$

where

$$\begin{aligned}
J_1&=J-\Gamma_2+\tfrac{1}{2}\Gamma^S\\
J_2&=(J-\Gamma_2-\tfrac{1}{2}\Gamma^S)\cos^2\varphi_{\mathrm{LTT}}-(J-\Gamma_1+\Gamma_2-\tfrac{1}{2}\Gamma^S)\sin^2\varphi_{\mathrm{LTT}}+\tfrac{1}{2}d\sin 2\varphi_{\mathrm{LTT}}\\
J_3&=-(J-\Gamma_2-\tfrac{1}{2}\Gamma^S)\sin^2\varphi_{\mathrm{LTT}}+(J-\Gamma_1+\Gamma_2-\tfrac{1}{2}\Gamma^S)\cos^2\varphi_{\mathrm{LTT}}+\tfrac{1}{2}d\sin 2\varphi_{\mathrm{LTT}}\\
J_4&=-\Gamma_1-\tfrac{1}{2}\Gamma^S\\
J_5&=\tfrac{1}{2}\Gamma^S\cos 2\varphi_{\mathrm{LTT}}+\tfrac{1}{2}d\sin 2\varphi_{\mathrm{LTT}}+\Gamma_1\sin^2\varphi_{\mathrm{LTT}}\,,
\end{aligned} \tag{68}$$

with $z=4$ and $S=1$. The zone-center spin-wave gaps with the in-plane and out-of-plane modes are obtained as

$$\varepsilon_i(0)\approx zS\left[4J\frac{1}{z}(A^{aa}-A^{cc})\right]^{1/2},\qquad \varepsilon_o(0)\approx zS\left[4J\frac{1}{z}(A^{aa}-A^{bb})\right]^{1/2}, \tag{69}$$

in the LTO phase, and as

$$\varepsilon_i(0)\approx zS\left[4J\frac{1}{z}(A^{yy}-A^{xx})\right]^{1/2},\qquad \varepsilon_o(0)\approx zS\left[4J\frac{1}{z}(A^{yy}-A^{zz})\right]^{1/2}, \tag{70}$$

in the LTT phase. Using the observed values of the in-plane and out-of-plane gaps[10] and $J=30$ meV,[10,25] we can estimate the magnitude of the single-ion anisotropies from Eq. (69) and Eq. (70): $(A^{aa}-A^{cc})\sim 0.13$ meV and

$(A^{aa}-A^{bb})\sim 0.55$ meV for the LTO phase and $(A^{yy}-A^{xx})\sim 0.04$ meV and $(A^{yy}-A^{zz})\sim 0.51$ meV for the LTT phase.

VI. CONCLUSIONS

We have examined the magnetic behaviors of cuprates and nickelates with low crystal symmetry. In La_2NiO_4, the spin arrangement is determined by the single-ion anisotropy. The weak ferromagnetism is derived when the determined spin arrangement can get the energy gain by the DM interaction: the weak ferromagnetism in the LTT phase and the antiferromagnetism without the spin canting in the LTO phase are explained by the different spin arrangements determined due to the different single-ion anisotropy. Generally speaking, in the insulating antiferromagnetic materials, the neighboring magnetic ions are separated by ~ 4 Å from each other by nonmagnetic ions. Due to hybridization of orbitals at this distance, the kinetic energy and Coulomb interaction can lead to the anisotropic exchange interactions of superexchange and direct-exchange mechanisms. On the other hand, the procedure of getting the single-ion anisotropy is carried out within each magnetic ion involved in the low-symmetry complex. Because of this difference, the strength of the single-ion anisotropy overwhelms the strength of the anisotropic exchange interactions of superexchange and direct-exchange mechanisms. The single-ion anisotropy plays an essential role in the construction of the spin structure of insulating antiferromagnetic materials. The weak ferromagnetism in the ordinary Dzyaloshinski-Moriya antiferromagnets emerges in the spin systems which involve the single-ion anisotropy. Moriya[13] has provided the microscopic mechanism of the exchange interaction which is responsible for the weak ferromagnetism. The weak ferromagnetism emerges in the cooperation of this DM interaction and the single-ion anisotropy.

The weak ferromagnetism of distorted cuprates must be treated as a distinct class of magnetism, not as a phenomenon in the ordinary Dzyaloshinski-Moriya antiferromagnets, because the Cu spin system does not involve the single-ion anisotropy. The weak ferromagnetism of distorted cuprates emerges in the competition between the DM and pseudodipolar interactions. The weak ferromagnetism requires the winning of the DM interaction. We have discussed that the effect of multiorbitals is essential for the emergence of weak ferromagnetism in distorted cuprates.

We have calculated the spin-wave excitation spectra in the distorted CuO_2 plane and NiO_2 plane. In cuprates, the spin-wave gaps are given by the exchange anisotropies; the in-plane spin-wave gap is provided by the anisotropic-exchange interactions of superexchange mechanism and the out-of-plane spin-wave gap is provided by the anisotropic-exchange interactions of direct-exchange mechanism. In nickelates, the spin-wave gaps are given by the single-ion anisotropy. Thus, we can understand naturally the structural dependence of the spin-wave gaps in cuprates and also the difference of the structural dependence of the spin-wave gaps between nickelates and cuprates.

ACKNOWLEDGMENTS

We would like to thank Professor Y. Endoh, Dr. K. Yamada, and Dr. K. Nakajima for providing experimental data for La_2NiO_4 prior to publication and for valuable discussions. We would also like to thank Professor M. Sato for instructive discussions on the neutron-scattering experiments for La_2CuO_4 and $La_{1.65}Nd_{0.35}CuO_4$. This work was supported by a Grant-in-Aid for Scientific Research on Priority Areas from the Ministry of Education, Science, and Culture of Japan.

[1] D. Vaknin, S. K. Sinha, D. E. Moncton, D. C. Johnston, J. M. Newsam, C. R. Safinya, and H. E. King, Jr., Phys. Rev. Lett. **58**, 2802 (1987).

[2] M. K. Crawford, R. L. Harlow, E. M. McCarron, and W. E. Farneth, Phys. Rev. B **44**, 7749 (1991).

[3] J. Rodríguez-Carvajal, J. L. Martínez, J. Pannetier, and R. Saez-Puche, Phys. Rev. B **38**, 7148 (1988).

[4] G. Burns, F. H. Dacol, D. E. Rice, D. J. Buttrey, and M. K. Crawford, Phys. Rev. B **42**, 10 777 (1990).

[5] J. Rodríguez-Carvajal, M. T. Fernández-Díaz, and J. L. Martínez, J. Phys. Condens. Matter **3**, 3215 (1991).

[6] K. Fukuda, S. Shamoto, M. Sato, and K. Oka, Solid State Commun. **65**, 1323 (1988); T. Thio, T. R. Thurston, N. W. Preyer, P. J. Picone, M. A. Kastner, H. P. Jenssen, D. R. Gabbe, C. Y. Chen, R. J. Birgeneau, and A. Aharony, Phys. Rev. B **38**, 905 (1988); M. A. Kastner, R. J. Birgeneau, T. R. Thurston, P. J. Picone, H. P. Jenssen, D. R. Gabbe, M. Sato, K. Fukuda, S. Shamoto, Y. Endoh, K. Yamada, and G. Shirane, *ibid.* **38**, 6636 (1988); T. Thio, C. Y. Chen, B. S. Freer, D. R. Gabbe, H. P. Jenssen, M. A. Kastner, P. J. Picone, N. W. Preyer, and R. J. Birgeneau, *ibid.* **41**, 231 (1990).

[7] S. Shamoto, T. Kiyokura, M. Sato, K. Kakurai, Y. Nakamura, and S. Uchida, Physica C **203**, 7 (1992).

[8] B. Keimer, R. J. Birgeneau, A. Cassanho, Y. Endoh, M. Greven, M. A. Kastner, and G. Shirane, Z. Phys. B **91**, 373 (1993).

[9] M. K. Crawford, R. L. Harlow, E. M. McCarron, W. E. Farneth, N. Herron, H. Chou, and D. E. Cox, Phys. Rev. B **47**, 11 623 (1993).

[10] K. Yamada, M. Arai, Y. Endoh, S. Hosoya, K. Nakajima, T. Perring, and A. Taylor, J. Phys. Soc. Jpn. **60**, 1197 (1991); K. Yamada, T. Omata, K. Nakajima, S. Hosoya, T. Sumida, and Y. Endoh, Physica C **191**, 15 (1992); S. Hosoya, T. Omata, K. Nakajima, K. Yamada, and Y. Endoh, *ibid.* **202**, 188 (1992); K. Nakajima, Ph.D. thesis, Tohoku University 1992; K. Nakajima, K. Yamada, S. Hosoya, T. Omata, and Y. Endoh, J. Phys. Soc. Jpn. **62**, 4438 (1993).

[11] C. J. Peters, R. J. Birgeneau, M. A. Kastner, H. Yoshizawa, Y. Endoh, J. Tranquada, G. Shirane, Y. Hidaka, M. Oda, M. Suzuki, and T. Murakami, Phys. Rev. B **37**, 9761 (1988).

[12]I. E. Dzyaloshinski, J. Phys. Chem. Solids **4**, 241 (1958).
[13]T. Moriya, Phys. Rev. **120**, 91 (1960).
[14]D. Coffey, K. S. Bedell, and S. A. Trugman, Phys. Rev. B **42**, 6509 (1990).
[15]D. Coffey, T. M. Rice, and F. C. Zhang, Phys. Rev. B **44**, 10 112 (1991); *ibid.* **46**, 5884(E) (1992).
[16]L. Shekhtman, O. Entin-Wohlman, and A. Aharony, Phys. Rev. Lett. **69**, 836 (1992); L. Shekhtman, A. Aharony, and O. Entin-Wohlman, Phys. Rev. B **47**, 174 (1993); O. Entin-Wohlman, A. Aharony, and L. Shekhtman (unpublished).
[17]N. E. Bonesteel, Phys. Rev. B **47**, 11 302 (1993).
[18]W. Koshibae, Y. Ohta, and S. Maekawa, Phys. Rev. B **47**, 3391 (1993); *ibid.* **48**, 3580(E) (1993); W. Koshibae, Y. Ohta, and S. Maekawa, Phys. Rev. Lett. **71**, 467 (1993).
[19]T. Yildirim, A. B. Harris, O. Entin-Wohlman, and A. Aharony (unpublished).
[20]The expression of $g_{nn'}$ for cuprates given in Ref. 18 is incomplete: the factor $\frac{1}{2}$ in an equation corresponding to Eq. (10) for $n \neq n'$ was missing. This was pointed out by L. Shekhtman, O. Entin-Wohlman, and A. Aharony, Phys. Rev. Lett. **71**, 468 (1993).
[21]W. Low, in *Solid State Physics* (Academic, New York, 1960), Suppl. 2, p. 77.
[22]S-W. Cheong, J. D. Thompson, and Z. Fisk, Physica C **158**, 109 (1989).
[23]A. K. McMahan, Richard M. Martin, and S. Satpathy, Phys. Rev. B **38**, 6650 (1988); M. S. Hybertsen, E. B. Stechel, M. Schluter, and D. R. Jennison, *ibid.* **41**, 11 068 (1988); S. B. Bacci, E. R. Gagliano, R. M. Martin, and J. F. Annet, *ibid.* **44**, 7504 (1990).
[24]K. B. Lyons, P. A. Fleury, J. P. Remeika, A. S. Cooper, and T. J. Negran, Phys. Rev. B **37**, 2353 (1988); R. T. Collins, Z. Schlesinger, M. W. Shafer, and T. R. McGuire, *ibid.* **37**, 5817 (1988); R. R. P. Singh, P. A. Fleury, K. B. Lyons, and P. E. Sulewski, Phys. Rev. Lett. **62**, 2736 (1989).
[25]S. Sugai, M. Sato, T. Kobayashi, J. Akimitsu, T. Ito, H. Takagi, S. Uchida, S. Hosoya, T. Kajitani, and T. Fukuda, Phys. Rev. B **42**, 1045 (1990).

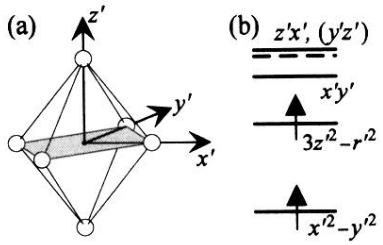

FIG. 1. (a) The NiO_6 octahedron and the $x'y'z'$-coordinate system. Open circles indicate O ions forming the octahedron; the Ni ion is located at the center. The shaded area is a section of the NiO_2 plane. (b) The crystal-field-level structure in the $x'y'z'$-coordinate system. Two holes are indicated by arrows.

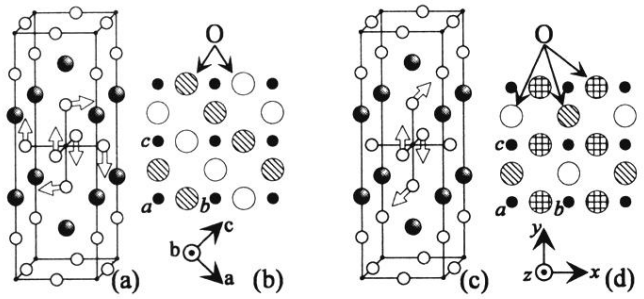

FIG. 2. (a) La_2CuO_4-type crystal structure in the LTO phase. The open arrows indicate the tilting of the octahedron. (b) The MO_2 (M = Cu, Ni) plane of the LTO phase: the O ions indicated by an open (hatched) circle are tilted up (down) out of the plane. (c) As in (a), but for the LTT phase. (c) As in (b), but for the LTT phase. The checked circles indicate the O ions remain in the plane.

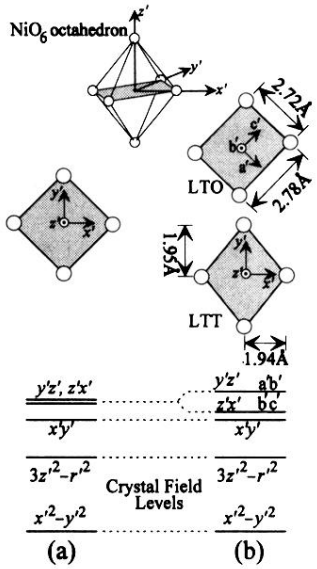

FIG. 5. Distortions of the NiO_6 octahedron in the LTO and LTT phases (Ref. 5), and changes in the crystal-field levels due to symmetry reduction. (a) The crystal-field-level structure for the undistorted NiO_6 octahedron: the $z'x'$ and $y'z'$ levels are degenerate because the cross section in the $x'y'$ plane is square for the octahedron with the D_{4h}-group symmetry. (b) The crystal-field-level structure for the distorted NiO_6 octahedron in the LTO and LTT phases: the degeneracy between the $z'x'$ and $y'z'$ levels is lifted because the octahedron has the D_{2h}-group symmetry where the crossection in the $x'y'$ plane is rectangular in the LTO phase and diamonds in the LTT phase.